Imprinting of nematic order at polymer network surfaces as a function of cross-link density

Karl R. Amundson
Bell Laboratories, Lucent Technologies, 600 Mountain Avenue, Murray Hill, New Jersey 07974
(Received 1 July 1998)

The effect of polymer structure on imprinting of nematic order on the surface of cross-linked polymer networks was studied. Polymer surfaces were formed in contact with a nematic phase by polymerization-induced phase separation in a nematic solvent. Nematic order imprints upon the interface, giving an easy axis for nematic anchoring. Surface imprinting diminished with decreasing cross-link density of the polymer network. This trend coincides with an increase in monomeric motion, as shown by a simple argument. This is an example of crossover from solidlike to liquidlike behavior in a cross-linked polymer as the cross-link density is varied. Also, surface imprinting is important because it can affect electro-optical properties of dispersions of polymers and liquid crystals made by polymerization-induced phase separation. [S1063-651X(99)07901-5]

PACS number(s): 42.70.Df

I. INTRODUCTION

Rubbery, amorphous polymer networks exhibit both solidlike and liquidlike characteristics. Constituent elements undergo molecular reorientation and translation, albeit restricted. On the other hand, because of the far-reaching extent of covalent bond pathways, polymer networks resist shear deformation, a characteristic in common with solids. As the density of cross links in a network decreases, motion of constituent elements becomes less restricted and the solidlike properties diminish. Macroscopic manifestations include a decrease in the elastic modulus and an increase in the degree of swelling in a good solvent [1,2]. NMR line shapes narrow with decreasing cross-link density as dipolar or other tensorial interactions are more completely averaged by internal motion [3,4]. In this work, crossover from solidlike to liquidlike behavior upon decreasing the cross-link density is demonstrated in yet another arena, that being anchoring energetics of liquid crystals at polymer network surfaces.

The surfaces studied in this work are formed upon polymerization-induced phase separation of a mixture of monomers and a liquid crystal. In a previous publication [5] it was shown that because the polymer network is formed while in contact with a nematic liquid crystal, nematic order can be imprinted onto the polymer network at interfaces. It is useful at this point to review some relevant previous findings.

Surface anchoring arises because the interfacial energy is a function of the orientation of the nematic near the interface. The anisotropic component is called the surface anchoring energy $w(\mathbf{n};\nu,\xi)$, where $\mathbf{n}$ is the nematic director, ν is the surface normal, and ξ indicates a special in-plane surface direction (see Fig. 1). w is typically small, and is often on the order of 10^{-2} to 10^{-4} times the average interfacial energy. Whether a liquid crystal prefers to orient with the director, $\mathbf{n}$, normal to the interface (*homeotropic* anchoring), in the plane of the interface (*homogeneous* anchoring), or along a tilted direction or directions depends upon subtle interactions that are not well understood. In a previous report, surface anchoring of a liquid crystal (TL205, E. Merck) at acrylate polymer network surfaces created by polymerization-induced phase separation was studied [6]. That work showed that surface anchoring is very sensitive to the polymer side group. Using acrylates with alkyl side groups, a temperature-induced anchoring transition was discovered. Anchoring is homeotropic below and homogeneous above an anchoring transition temperature, T_t. T_t is near the nematic-to-isotropic transition temperature when the polymer side group is a long, straight alkyl chain and is much lower when the alkyl side group is short, branch, or cyclic. T_t can be adjusted across nearly the entire nematic temperature range by judicious selection of polymer side group and by mixing of side groups.

The ability to tailor the anchoring energy by making small changes in the side group chemistry permitted studying the effect of anchoring without significantly changing the resulting morphology. In subsequent work, this was important for demonstrating imprinting of nematic order at polymer network surfaces created by polymerization-induced phase separation [5]. Pairs of polymer-dispersed liquid-crystal

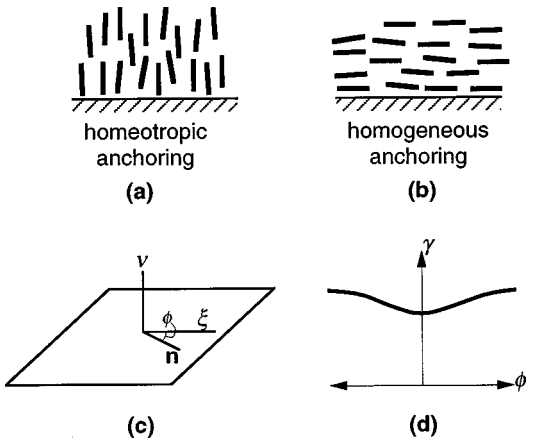

FIG. 1. (a) Homeotropic and (b) homogeneous anchoring are illustrated. Rodlike mesogens are shown above a surface. Homogeneous anchoring at an isotropic surface is degenerate and all in-plane director orientations have the same surface energy. At an anisotropic surface (c) homogeneous anchoring can be nondegenerate and certain in-plane orientations give a lower surface energy γ than other orientations, as illustrated in (d). ϕ is the angle between the in-plane director and the orientation that gives the minimum surface energy, denoted by the easy axis, ξ.

(PDLC) films were made. Film formation begins with an isotropic mixture of monomer and liquid crystal between two substrates. Upon photopolymerization, the mesogen becomes supersaturated and nematic drops form. Solidification of the polymer network halts the coalescence of the drops into large structures. Confocal microscopy showed the nematic component to form discrete drops within a continuous polymer matrix [7]. The drop size can be controlled by various factors, and are typically about 1–5 μm. An external field is applied across one film that is sufficiently strong to align the nematic in the newly forming drops but too weak to alter structure. The other film is formed in the absence of a field and so the director in each drop adopts a pattern that minimizes the sum of nematoelastic distortion and surface energies. Subsequent differences in optical and electrical properties between the two films were found when anchoring was homogeneous but not when anchoring was homeotropic, showing that the memory was held at the surface of the drops [5]. The fact that imprinting survived excursions through an anchoring transition and isotropization of the nematic argued that imprinting was not due to surface-adsorbed mesogens, but instead due to anisotropy imposed upon the polymer network at the drop surfaces. Also, surface imprinting occurred during polymerization, but after polymerization a new nematic director orientation could not be imprinted. This supports a model where surface anisotropy is held by cross-linking of the polymer network, so that once the network has cross-linked, imprinting of a new nematic director orientation is not possible. In this paper, the connection between imprinting and the polymer network structure is explored. Imprinting diminishes as the cross-link density is reduced. While imprinting is possible at solid surfaces, liquids cannot retain long-term memory. In this light, these experiments provide another example of crossover from solidlike to liquidlike behavior for a polymer network as a function of cross-link density.

II. EXPERIMENT

PDLC films were made from a mixture of 70–80 wt. % liquid crystal (TL205, EM Industries) and the remainder a uv-curable acrylate monomer mixture. TL205 is a mixture of halogenated biphenyls and terphenyls with aliphatic tails of lengths two to five carbons [8]. The choice for monofunctional acrylate is driven by the need for homogeneous anchoring at the temperature of film formation ($\sim$23 °C) in order to permit imprinting. In addition, an experimentally accessible anchoring transition temperature is desirable because the transition temperature is a sensitive probe of surface composition. A mixture of three parts (by weight) isobornyl acrylate and one part *n*-octyl acrylate was used as the monofunctional acrylate component because it gives rise to an anchoring transition near 14 °C and anchoring is homogeneous at room temperature. A trifunctional acrylate (1,1,1-trimethylol propane triacrylate) was added to provide cross-links to the polymer network. The ultraviolet (uv) sensitive photoinitiator (Darocur 1173, Ciba) was added to this monomer mixture at a concentration of 1.5 wt. %. The cross-link density of the polymer network was controlled by the choice of the trifunctional acrylate concentration.

In each experiment, the mixture was placed between pairs of indium-tin-oxide-coated glass plates separated by $\sim$14 μm, then cured with uv light ($\sim$14 mW/cm^2, 8–10 min). Two films were formed simultaneously. Across one film, a sinusoidal (1 kHz) voltage (26 V_{rms}) was applied throughout photopolymerization, and it is referred to as the field-cured film. The other, with no voltage applied during photopolymerization, is referred to as the reference film. The low scattering power after the onset of phase separation in the field-cured film compared to the reference film showed that the director was well aligned by the field. A series of film pairs were made using 80 wt. % liquid crystal and variable concentrations of trifunctional acrylate. At low cross-link density, if the liquid-crystal fraction was held at 80 wt. %, the drops formed before the matrix became sufficiently solid, and some drops coalesced to form large features. In these cases, additional films were made using a lower liquid-crystal fraction until the film morphology appeared similar (by optical microscopy) to films formed from mixtures with the higher cross-link density.

The degree of nematic director alignment along the substrate normal was probed by dielectric measurements. Electrical impedance across each film was determined by measuring the amplitude and phase of current passing through the film at 1 kHz while applying a small 1-kHz voltage signal as described in Ref. [5]. The impedance was also measured when the nematic was well aligned by a large-amplitude 60-Hz voltage. The 60-Hz aligning voltage was mixed with a 1-kHz test voltage, and the current at 1 kHz only was measured. Good alignment with the field was verified by observing that electrical and optical properties of the film did not change upon increasing the applied voltage. The film temperature during dielectric measurements was controlled using a Mettler FP82 hot stage with cold nitrogen gas flow.

III. RESULTS AND DISCUSSION

For all films studied, the impedance is reactive (current-voltage phase angle of 87°–90°) at the probe voltage frequency of 1 kHz, so to a good approximation the impedance can be considered purely capacitive. The capacitance of the film can be expressed as

$$C = \frac{\varepsilon_{\mathrm{eff}} A}{d}, \tag{1}$$

where A is the surface area of the overlapping parts of the electrodes, d is the gap thickness, and $\varepsilon_{\mathrm{eff}}$ is the effective dielectric constant. The capacitance at zero excitation voltage (C_0) and the capacitance while applying an aligning voltage sufficient to fully align the nematic component (C_∞) were recorded. The ratio of these two is a convenient measure because it is independent of the film geometry, and is given by the ratio of the effective dielectric constant under the relaxed and aligned conditions, ε_0 and ε_∞, respectively:

$$\frac{C_0}{C_\infty} = \frac{\varepsilon_0}{\varepsilon_\infty}. \tag{2}$$

The effective dielectric constant is a function of the polymer dielectric constant and of the dielectric tensor of the nematic

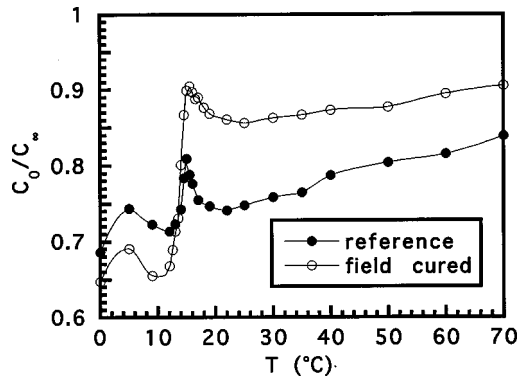

FIG. 2. C_0/C_∞ for the field cured and reference films made with 13.5 wt. % trimethylol propane triacrylate.

in the drops. Because the dielectric anisotropy of the liquid crystal is positive (ε_{par}-$\varepsilon_{\text{perp}}$=5.0 at 24 °C), the dielectric constant of the film is greatest when the nematic director is aligned with the electric field. ε_∞ is thus an upper bound on the dielectric constant at any given temperature. In zero field, the director within each drop orients according to the drop shape and surface anchoring forces, and so the ratio C_0/C_∞ is less than unity. For example, if the director orientation distribution is globally isotropic in zero field, then the ratio C_0/C_∞ should be about 0.7 at room temperature, based upon the dielectric constants of the liquid crystal and polymer matrix. [This ratio heads toward unity as the film is heated toward the nematic-to-isotropic transition temperature (T_{NI}) because the dielectric anisotropy diminishes as T_{NI} is approached.] A bias in the director distribution toward the film normal will increase C_0/C_∞.

Figure 2 shows the capacitance ratio for the pair of PDLC films prepared using 13.5 wt. % trifunctional acrylate in the matrix formulation. Above the anchoring transition temperature, the field-cured film has a significantly larger capacitance ratio, indicating a greater tendency for alignment with the substrate normal in zero field. This is a result of imprinting of the early nematic director orientation at the drop surfaces. The easy axis is aligned along the film normal in the field-cured film, while in the reference film nematic order is imprinted at each drop surface according to each drop shape. This biases the director distribution function toward greater alignment along the substrate normal in the field-cured film compared to the reference film. Below T_t anchoring is homeotropic and one would expect the capacitance of the two films to be similar. Instead, the capacitance ratio of the field-cured film is slightly lower than the reference film. The reason for this is unknown. It is possible that there are complexities to anchoring at these surfaces that are not well understood. Also, transients at the lowest experimental temperatures become quite long, and so the data at 0 °C are not very reliable. It should be noted that the effect of orienting the director during film formation could also be seen in the forward light transmittance through the films. The field-cured film was less scattering than the reference film across the range where anchoring is homogeneous. However, because the forward-scattering measurements added little beyond the impedance measurements and were susceptible to thickness differences between films, scattering data are not presented.

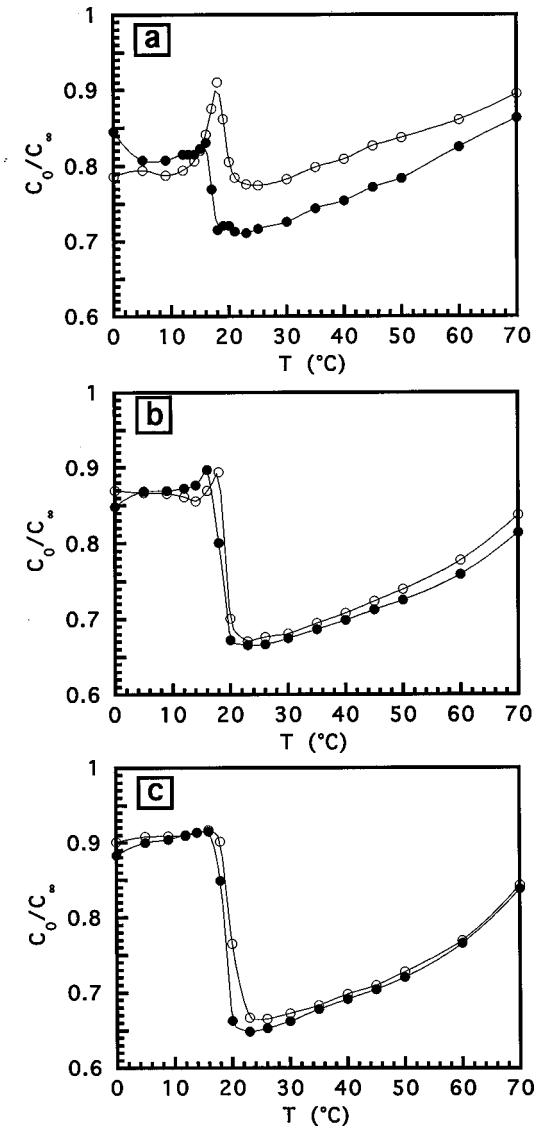

FIG. 3. C_0/C_∞ for the field cured and reference films made with (a) 4.0, (b) 2.0, and (c) 1.0 wt. % trimethylol propane triacrylate. Solid points are for the reference films and the open circles are for the field-cured films.

Additional pairs of films were made using the same formulation but with lower trifunctional acrylate concentrations. Figures 3(a)–3(c) show C_0/C_∞ for films that contain 4.0, 2.0, and 1.0 wt. % trifunctional acrylate with the liquid-crystal fraction held at 80 wt. %. For the film with 4.0 wt. % trifunctional acrylate, over the temperature range where anchoring is homogeneous, the capacitance ratio is greater for the field-cured film than the reference film. However, the enhancement is noticeably smaller than in the film with 13.5 wt. % trifunctional acrylate in the monomer mixture. When the trifunctional acrylate concentration was reduced to 2.0 wt. % or below, there was no significant distinction between the field-cured and reference films.

Varying the concentration of trifunctional acrylate not only changes the cross-link density of the polymer network in the photopolymerized film, it also changes the drop size. This is because the growth of the polymer network is facilitated by the presence of the trifunctional acrylate. While the films formed with 13.5 and 4.0 wt. % trifunctional acrylate

gave films with an approximately similar drop size (as estimated by optical microscopy), the drops were noticeably larger in the films made with 2% and 1% trifunctional acrylate. In fact, the drop sizes were significant compared to the film thickness (~ 14 μm) so that the drops become statistically flattened along the axis normal to the substrates, as revealed by the capacitance data. Consider an oblate nematic drop with only a mild distortion from sphericity and a short axis perpendicular to the film substrates. In normal anchoring, the director will have a greater presence along the film normal compared to the equiaxial texture in a spherical drop. In planar anchoring, the nematoelastic distortion energy is minimized when the director is aligned along a long axis of the drop, which in this case is in-plane. In this way, a statistical bias toward a shortening of the drop axes along the substrate normal will give an anomalously high capacitance in normal anchoring and an anomalously low capacitance in planar anchoring. This effect becomes apparent for the two films made with 2% and 1% trifunctional acrylate [see Figs. 3(b) and 3(c)], where the capacitance ratio drops sharply upon heating through T_t.

To verify that the reduction in the difference between the field-cured and reference films with decreasing cross-link density was due to changes in the polymer structure and not the increase in drop size, a second set of films was formed with 2% and 1% trifunctional acrylate but with less liquid crystal. The decrease in liquid-crystal fraction causes phase separation to occur later in the polymerization process, bringing the drop size back down [7]. Films with drop size distributions similar to films with the larger cross-link fraction were developed by reducing the liquid-crystal fraction from 80 wt. % down to 75 and 70 wt. % for the films with 2% and 1% trifunctional acrylate, respectively. Figures 4(a) and 4(b) show the capacitance ratio for these two films. The anomalous behavior associated with large drops discussed in the preceding paragraph is eliminated. But more to the point, there is no significant difference between the field-cured and reference films. It is important to note that the anchoring transition, indicated by the spike and discontinuity in the capacitance ratio, varied very little among all these samples. This showed that the surface composition is similar in all the films.

The ability to imprint long-term memory into a polymer network relies upon restrictions in reorientation and translation of monomers comprising the network strands. As the cross-link density diminishes, the number of available configurations increases, and so any effects of memory should weaken. Eventually, so many configurations are available that the surface will behave like a simple liquid and not exhibit memory.

Dynamics of strands in a polymer network is complex because each network strand interacts with numerous neighboring strands and the end points of the strands themselves move. A useful simplification for the purpose at hand is to assume that the dynamics of monomers in a strand are governed mostly by the end-to-end vector of the strand. In this approximation, motion is hindered primarily by the separation of the end points of the strand, where a strand is defined as a sequence of monomers between cross-link sites (see Fig. 5). Only strands that are coupled into the network at both ends are considered. Reorientational dynamics under this approximation and the additional approximation that the end

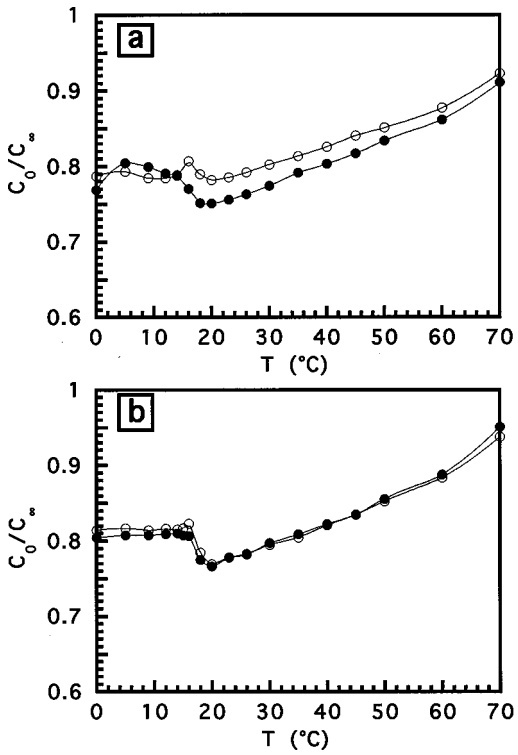

FIG. 4. C_0/C_∞ for the field cured and reference films made with (a) 2.0 (b) 1.0 wt% trimethylol propane triacrylate. The liquid crystal fraction is 75 wt% in the former case and 70 wt% in the latter. Solid points are for the reference films and the open circles are for the field-cured films.

points are fixed was worked out by Cohen-Addad [3,4]. A network strand under consideration is divided into Kuhn segments in the usual manner [9], and the orientational distribution function for each Kuhn segment is given by

$$P(\theta)=\frac{1}{4\pi}\frac{\alpha}{\sinh(\alpha)}\exp[\alpha\cos(\theta)], \tag{3}$$

where

$$\alpha=\frac{3ar_c}{\sigma_c^2}.$$

P is the time-averaged probability distribution of a Kuhn segment orientation and θ is the polar angle with respect to the end-to-end vector $\mathbf{r}_c$ of the network strand. a is the Kuhn segment length, r_c the magnitude of $\mathbf{r}_c$ and σ_c^2 the mean-

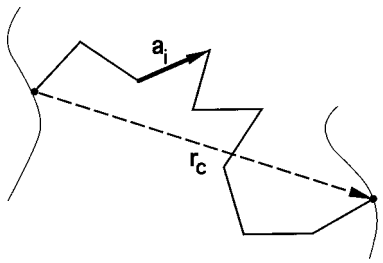

FIG. 5. A hypothetical polymer network strand composed of a series of freely jointed monomers denoted by a set of vectors $\mathbf{a}_i$ and with an end-to-end vector $\mathbf{r}_c$.

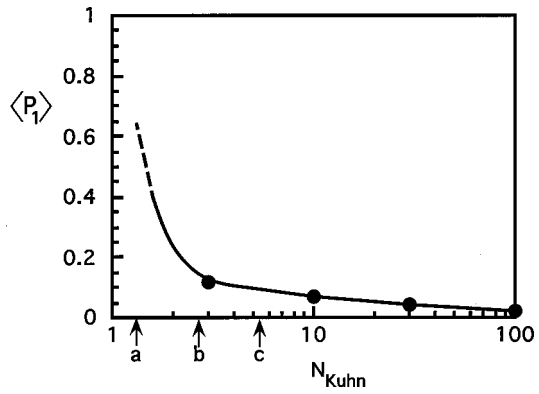

FIG. 6. First angular moment of the orientation of a Kuhn segment (denoted by vector $\mathbf{a}_i$ in Fig. 5) as a function of the number of Kuhn segments N_{Kuhn} in a strand. The arrows marked *a*, *b*, and *c* denote the average N_{Kuhn} for films made with 4.0, 2.0, and 1.0 wt. % trimethylol propane triacrylate. The average strand length for the film made with 13.5 wt. % trimethylol propane triacrylate is less than one Kuhn segment.

square end-to-end vector of the segment. If the strands are not strained, the average magnitude of r_c is $N_c^{1/2}a$ and σ_c^2 is $N_c a^2$, where N_c is the number of Kuhn segments between cross-links. α is then equal to $3/N_c^{1/2}$, and the angular distribution is completely determined by the number of Kuhn segments in the strand:

$$P(\theta)=\frac{1}{4\pi}\frac{3}{N_c^{1/2}\sinh(3/N_c^{1/2})}\exp\left(\frac{3}{N_c^{1/2}}\cos(\theta)\right). \quad (4)$$

Segments in a strand made up of a small number of Kuhn segments will exhibit strongly restricted reorientation, and motion becomes less restricted as the number of Kuhn segments in a strand increases. Figure 6 shows the first angular moment (Legendre polynomial, P_1) of the distribution function of Eq. (4). $\langle P_1\rangle$ drops to zero asymptotically with increasing strand length.

The average network segment length estimated from the stoichiometry of each monomer mixture, and assuming ideal network formation, is shown in Table I [10]. Also shown in Table I is the number of equivalent Kuhn segments in an average network strand. The characteristic ratio of 9, typical of acrylate polymers, was used [11]. Corresponding positions for three of the four compositions are indicate in Fig. 6 (the film with the highest cross-link density has an average strand length less than a Kuhn segment). Recall that the effect of imprinting diminished to below detectable levels in going from 4 to 2 wt. % cross-linking fraction in the matrix mixture. At the same time, the degree of internal motion of the polymer network increases dramatically over this range, as reflected in the rapid decrease in the first moment of the Kuhn segment orientational distribution function between arrows labeled *a* and *b* in Fig. 6.

TABLE I. Number of monomers, N_e, and equivalent number of Kuhn segments, N_{Kuhn} in an average network strand.

Trifunctional acrylate in monomer mixture (wt. %)	N_e	N_{Kuhn}
13.5	3.1	0.3
4	11.6	1.3
2	23.7	2.6
1	47.5	5.3

The scenario built from these observations is the following. At the drop interface, while a polymer network forms, monomers at the drop interface interact with mesogens in the nematic phase. Configurations where functional groups are oriented or spatially arranged to give favorable interactions with nearby mesogens are trapped by cross-linking. In a highly cross-linked network, the favorable configurations are revisited often because the number of available configurations is limited, while in a loosely cross-linked network the number of configurations visited can be so large that there is very little memory of any configuration favorable to a previous direction of nematic order.

It is worth noting that the anisotropy required to induce an easy axis at a polymer network surface can be extremely slight. In order to induce a change in the orientation of the director pattern inside a nematic drop, the azimuthal energy difference, w_ϕ, between orthogonal surface orientations need only overcome the bulk nematoelastic energy difference between low- and high-energy orientations in the drop:

$$w_\phi R^2 \sim KR(\alpha^2-1)^{1/2}, \quad (5)$$

where R is the drop radius, K is the elastic constant, and α is the drop aspect ratio [12,13]. This gives a w_ϕ on the order of 10^{-2}–10^{-3} erg/cm^2, or about 10^{-3}–10^{-4} times the interfacial energy typical of organic-organic interfaces ($\sim$10 erg/cm^2). In principle, this slight difference could come about from a very small anisotropy in surface structure.

In this scenario, imprinting of nematic order at a network surface is akin to molecular recognition through templating of polymer networks [14]. Molecular templating in polymer networks is commonly reported as a bulk phenomenon, where a polymer network is formed in the presence of, typically, a complex molecule acting as a template. The template molecule is removed, and later the polymer exhibits a special affinity for that molecule. For the studies presented here, the direction of nematic order is imprinted instead, but some of the principles may be similar.

The observations reported here are important on technological grounds, especially because, over the past decade, a variety of polymer/liquid-crystal composite materials with interesting electro-optical properties have been developed using polymerization-induced phase separation. One example is the PDLC morphology formed in this study. PDLC films exhibit a scattering power that can be electrically varied [12,15,16] and are proposed for use in flat-panel displays, switchable photonic devices [17–19], and are used as switchable architectural windows. Other examples include bicontinuous polymer/liquid-crystal composites such as polymer stabilized cholesteric textures [16,20–22] and polymer-modified ferroelectric liquid-crystal films [23–25] each with their unique electro-optic properties. Because of the large surface-to-volume ratio of these composites, surface anchoring, including an imprinted easy axis, is crucial to device performance [6,16,26,27].

IV. CONCLUSIONS

Surface imprinting of nematic order at polymer network surfaces created by polymerization-induced phase separation was studied. Surface imprinting was shown to be most strong in films where the cross-link density was highest and imprinting became undetectably small when the cross-link density was low. Over the range where surface imprinting diminished, the motion of monomers in an average chain segment was estimated to increase dramatically. This is a new example of crossover from solidlike to liquidlike character for a polymer network achieved by varying the cross-link density. Also, surface imprinting is important because it affects the electro-optical properties of films incorporating liquid crystal.

ACKNOWLEDGMENT

The author thanks Mohan Srinivasarao for helpful discussions.

[1] L. R. G. Treloar, *The Physics of Rubber Elasticity* (Oxford University Press, New York, 1958), Chap. 9.
[2] T. Tanaka, Phys. Rev. Lett. **40**, 820 (1978).
[3] J. P. Cohen-Addad, J. Chem. Phys. **64**, 3438 (1976).
[4] J. P. Cohen-Addad, J. Phys. (Paris) **43**, 1509 (1982).
[5] K. Amundson, Phys. Rev. E **58**, 3273 (1998).
[6] K. Amundson and M. Srinivasarao, Phys. Rev. E **58**, R1211 (1998).
[7] K. Amundson, A. van Blaaderen, and P. Wiltzius, Phys. Rev. E **55**, 1646 (1997).
[8] D. Coates (private communication).
[9] P. J. Flory, *Statistical Mechanics of Chain Molecules* (Carl Hanser, New York, 1989).
[10] The calculation of the average network strand length assumes an ideal network without dangling ends and complete and homogeneous reaction of the monomers. Therefore the calculation gives only a rough approximation of the average strand length.
[11] The characteristic ratio for a number of acrylates and methacrylates can be found in the *Polymer Handbook*, 3rd ed. by J. Brandrup and E. H. Immergut (Wiley, New York, 1989), Pt. VII, pp. 33–46. Values are typically between 7 and 10.
[12] P. S. Drzaic and A. Muller, Liq. Cryst. **5**, 1467 (1989).
[13] B.-G. Wu, J. H. Erdmann, and J. W. Doane, Liq. Cryst. **5**, 1453 (1989).
[14] G. Wulff, Angew. Chem. Int. Ed. Engl. **34**, 1812 (1995), and references therein.
[15] J. W. Doane, MRS Bull. **16**, 22 (1991).
[16] P. S. Drzaic, *Liquid Crystal Dispersions* (World Scientific, Teaneck, NJ, 1995).
[17] R. L. Sutherland, L. V. Natarajan, V. P. Tondiglia, and T. J. Bunning, Chem. Mater. **5**, 1533 (1993).
[18] R. L. Sutherland, V. P. Tondiglia, L. V. Natarajan, T. J. Bunning, and W. W. Adams, Appl. Phys. Lett. **64**, 1074 (1994).
[19] V. P. Tondiglia, L. V. Natarajan, R. L. Sutherland, T. J. Bunning, and W. W. Adams, Opt. Lett. **20**, 1325 (1995).
[20] D. K. Yang, L.-C. Chien, and J. W. Doane, Appl. Phys. Lett. **60**, 3102 (1992).
[21] D. K. Yang, J. L. West, L.-C. Chien, and J. W. Doane, J. Appl. Phys. **76**, 1331 (1994).
[22] C. N. Bowman and C. A. Guymon, MRS Bull. **22**, 15 (1997).
[23] C. A. Guymon and C. N. Bowman, Macromolecules **30**, 1594 (1997).
[24] H. Fujikake *et al.*, Jpn. J. Appl. Phys., Part 1 **36**, 6449 (1997).
[25] H. Furue *et al.*, Jpn. J. Appl. Phys., Part 1 **36**, 1517 (1997).
[26] J. H. Erdmann, S. Zumer, and J. W. Doane, Phys. Rev. Lett. **64**, 1907 (1990).
[27] K. Amundson, Phys. Rev. E **53**, 2412 (1996).